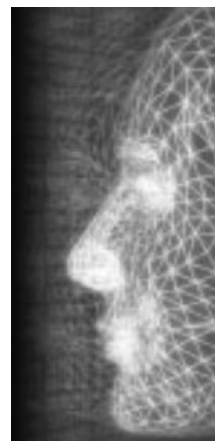


Inhomogeneous volumetric Laplacian deformation for rhinoplasty planning and simulation system

By Sheng-hui Liao*, Ruo-feng Tong, Jian-Ping Geng and Min Tang



This paper presents an intuitive rhinoplasty planning and simulation system, to provide high quality prediction of postoperative appearance, and design patient specific nose prosthesis automatically. The key component is a novel volumetric Laplacian deformation tool inspired by the state-of-the-art differential surface deformation techniques. Working on the volumetric domain and incorporating inhomogeneous material from CT data make the new approach suitable for soft tissue simulation. In particular, the system employs a special sketch contour driving deformation interface, which can provide realistic 3D rhinoplasty simulation with intuitive and straightforward 2D manipulation. When satisfied with the appearance, the change of soft tissue before and after simulation is utilized to generate the individual prosthesis model automatically. Clinical validation using post-operative CT data demonstrated that the system can provide prediction results of high quality. And the surgeons who used the system confirmed that this planning system is attractive and has potential for daily clinical practice. Copyright © 2010 John Wiley & Sons, Ltd.

KEY WORDS: individual prosthesis design; inhomogeneous material; rhinoplasty; soft tissue deformation; volumetric Laplacian

Introduction

The human face plays a key role in interpersonal relationships, and even very subtle malformation of facial proportions can strongly affect the appearance of a face and determine aesthetic aspects such as individual beauty. Therefore, planning of the operation and reliable prediction of soft tissue deformation are very important in view of a better preparation, shorter operation time, and improved surgical outcome.

There were many studies concentrated on the development of simulation tools for facial surgery as well as other type of soft tissue. The two most popular and widely used methods for deformation are mass-spring model and finite element method.¹ The mass-spring model is relatively simple to implement and has low computational complexity. But the simplicity comes

at the price of a few drawbacks, e.g., the system behavior depends on the way the spring network is set up; it is difficult to tune the spring stiffness to get desired behavior; and it cannot capture volumetric effects directly. In contrast, finite element method is a more biomechanical relevant model as derived directly from continuum mechanics for providing more accurate deformation result.² However, it is relatively complex to implement and computationally expensive.

In addition, most of those general simulation tools were driving by theory research instead of by the requirement of practical application, thus paid little attention to how to put the simulation result into actual use. In particular, the shape of the nose is one of the most distinctive face features, and rhinoplasty, or surgery to reshape the nose, is one of the most frequently performed facial plastic surgery, which usually needs to design patient specific prosthesis that has a direct effect on postoperative aesthetic effects. This adds a challenging dimension to the problem, because standard nose prosthesis models are not suitable to be used

*Correspondence to: S.-h. Liao, State Key Laboratory of CAD&CG, Zhejiang University, Hangzhou 310027, P. R. China. E-mail: shliao@zju.edu.cn

directly for individual surgery. If using the traditional simulation mode, e.g., simulate soft tissue deformation caused by bone osteotomy and/or prosthesis, one needs to guess and modify the shape of the prosthesis model manually before soft tissue simulation. To achieve desired aesthetic effect, it may need many times of prosthesis modification—soft tissue simulation loops.

The motivation of this study is to investigate an intuitive and practical rhinoplasty planning and simulation system. We believe it is worth to focus on this most popular plastic surgery, and provide a solution which is truly helpful for daily clinical practice. The underlying techniques can also be adapted directly in other virtual and simulation tasks in computer graphics.

Design Consideration

There are commercially available packages which let the surgeon simulate the final nose shape, such as the AlterImage cosmetic surgery simulation system (Seattle Software Design). These packages work with 2D photograph, using image manipulation technique to alter the patient's nasal profile.³ However, such 2D image based planning aids are less than ideal, as both the surgeon and patient would prefer a full 3D system that allows for more realistic simulation and full spatial relationship of the nose and face from different views.

To address the problem, several studies developed 3D deformation tools, interacting with a texture-mapped surface model of the face.⁴ In particular, the free-form deformation (FFD) technique was used to drive the deformation. The main drawback of FFD is that the user has to manipulate with the control mesh, and it can be difficult to control the object shape under complex deformations, especially for detailed local deformations. Another drawback is the influence of the control point positions on the deformation. Dependent on the initial control lattice (mesh), some deformations cannot be achieved. Lee *et al.*⁵ presented a 3D feature-based volume morphing method for rhinoplasty. The system requires surgeons to specify several feature line segments on the head surface to control the reshaping of the nose. The volume morphing is also an embedding space warping technique and has some similar drawbacks as the FFD, thus lots of manual efforts are needed to achieve desired effect.

It is obvious that the 3D surgery simulation system is more attractive than the 2D image based system for both surgeons and patients. On the other hand, we observed that the manipulation of existing 3D deformation tools

seems too “flexible”, and not as intuitive as those 2D image based simulation tools, in particularly for the nose surgery. In addition, there is a break between the simulation and surgical practice, as pointed out in previous section, currently surgeons need to guess and reshape standard nose prosthesis for a specific patient according to the simulation result. In other words, the surgeons need past experience to form the correct correlation between the simulated results and the clinical surgery.

In order to bridge the gap and overcome the aforementioned deficiencies, this paper presents an intuitive computer assisted nose surgery system, to provide high quality prediction of the postoperative appearance, and design the patient specific prosthesis model automatically. The key component is a novel inhomogeneous volumetric Laplacian deformation method, which can preserve volumetric detail and take the underlying physical material into account. Loosely speaking, we manage to provide some kind of “what you see is what you get” effect, e.g., using an intuitive interface to design directly the 3D postoperative appearance first, then produce necessary surgical planning and individual prosthesis design, which can be exported to some reverse rapid prototyping equipment to build the required physical prosthesis. We believe that this is more convenient for the communication between the surgeon and patient to identify the desired outcome of surgery, and more useful to put the simulation result into actual use.

The remainder of this paper is organized as follows. Section 3 will introduce the volumetric Laplacian deformation technique. Section 4 describes the surgery planning and simulation system. Section 5 provides some experiments and clinical validation. Finally, concluding remarks are given in Section 6.

State-of-the-Art Surface Deformation

The study is inspired by the state-of-the-art surface deformation techniques based on differential representations, which have gained significant popularity recently for their robustness, speed, and ease of implementation.^{6–8} The main idea behind this family of deformation techniques is to use a surface representation that puts the local differential properties in focus, and to preserve these differential properties under deformation, aspiring to obtain an intuitive,

detail-preserving deformation result. Various techniques differ by the particular differential properties they use, and the two most famous are gradient-based representation⁷ and Laplacian-based representation.⁸

Despite the ability to preserve surface geometric detail, it should be noted that most of those surface based deformation methods do not take the volume of the object into account. As a result, self-intersections might happen during deformation, and in general the volume of the shape cannot be preserved. In other words, surface based methods are not well-suited for the modeling of soft tissue, because approximately 70 per cent of the human body is based on water and the overall volume should be maintained even during a large deformation. A natural solution to address this problem is to extend the surface based deformation methods to volume based approaches, and enforce volume preservation through an explicit construction of the interior of the shape, e.g., using volumetric mesh. In addition, working in the volumetric domain can further avoid local self-intersections, and achieve better deformation propagation.

Besides, it is important to note that most of these geometric deformation techniques ignore the properties of the underlying materials, and thus make it difficult to generate physically plausible deformations, especially for inhomogeneous objects such as soft tissue.

To address these problems, we present a novel inhomogeneous volumetric Laplacian deformation method, which can preserve volumetric detail and take the underlying physical material into account. Furthermore, it is very suitable for the reverse simulation configuration in this paper.

Volumetric Laplacian Deformation

The basic setup of our volumetric deformation technique is similar to the surface Laplacian editing.⁸ However, we are working in the volumetric domain instead of on the surface only. Let $M = (V, K)$ be a tetrahedral mesh, where $V = \{p_i \in R^3 | 1 \leq i \leq n\}$ is a set of vertices, and K is an abstract simplicial complex which contains all the vertex connectivity information: edges $\{i, j\}$, faces $\{i, j, k\}$, and tetrahedrons $\{i, j, p, q\}$. The Laplacian coordinate (LC) δ_i at vertex i ($1 \leq i \leq n$) is defined as follows:

$$\delta_i = D(p_i) = \sum_{j \in N(i)} w_{ij}(p_j - p_i) \quad (1)$$

where $N(i)$ is the index set of the 1-ring neighboring vertices of p_i , and w_{ij} is the weight of the edge (i, j) . Note that the operator D is linear and can be represented by an $n \times n$ sparse and symmetric matrix L , e.g., the discrete volumetric Laplacian operator

$$L_{ij} = \begin{cases} \sum_{k \in N(i)} w_{ik}, & \text{if } i = j \\ -w_{ij}, & \text{if } j \in N(i) \\ 0, & \text{otherwise} \end{cases} \quad (2)$$

so that $(\delta^{(x)}, \delta^{(y)}, \delta^{(z)}) = L(p^{(x)}, p^{(y)}, p^{(z)})$, where $\delta^{(x)}$ is the n -vector of x components of $D(p)$.

Thus, the key issue to extend the surface deformation to volumetric domain is the discrete volumetric Laplacian operator. However, unlike the surface Laplacian operator, there are only a few published studies that describe the volumetric Laplacian operator.⁹⁻¹¹ Meyer *et al.*⁹ first pointed out the volumetric edge weight is proportional to the cotangents of dihedral angles. Wang *et al.*¹⁰ deduced the volumetric operator based on a harmonic energy and set the edge weight as $w_{ij} = \frac{1}{12} \sum_{k=1}^n l_k \cot(\theta_k)$, where $l_k = l_{pq}$ is the length of opposite edge (p, q) to which edge (i, j) is against, and $\theta_k = \theta_{pq}$ is the dihedral angle, as shown in Figure 1. Liao *et al.*¹¹ recently deduced a material weighted volumetric Laplacian operator based on its basic definition $\Delta u \equiv \text{div}(\nabla u)$, and set the edge weight as $w_{ij} = \frac{1}{6} \sum_{k=1}^n l_k m_k \cot(\theta_k)$ where m_k is the mesh element stiffness parameter in each tetrahedron to take inhomogeneous material into consideration. But these weighting schemes do not take varying vertex densities into account, and may lead to unnatural deformation

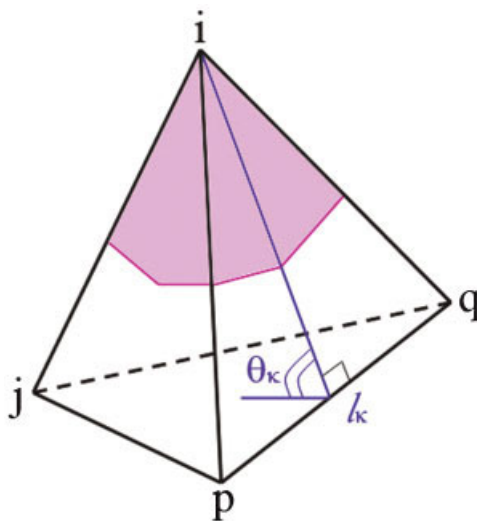


Figure 1. Illustration of volumetric Laplacian operator in a tetrahedron.

results for irregular meshes. To make the simulation as accurate as possible, we propose to employ additional per-vertex normalization weights $1/|\Omega_i|$ like the surface case,⁹ where $|\Omega_i|$ is the volume of Voronoi cell of vertex i , such as the pink region in Figure 1. Taken together, the normalized material weighted volumetric Laplacian operator can be formulated as

$$\Delta u_i = \frac{1}{|\Omega_i|} \sum_{j \in N(i)} \left(\frac{1}{6} \sum_{k=1}^n l_k m_k \cot(\theta_k) \right) (u_i - u_j) \quad (3)$$

Given the Laplacian coordinates $\delta^{(x)}, \delta^{(y)}, \delta^{(z)}$ of the mesh, the absolute coordinates can be reconstructed by solving the system $Lx = \delta^{(x)}$ (the same goes for y and z coordinates), provided with positional constraint conditions $p_k = c_k, k \in C$, where C denotes the set of indices of those vertices whose position is known. The form of soft constraints is used instead of hard constraints, by adding Equations $w_i x_i = w_i c_i$ to the system, where the weight $w_i > 0$ can be used to tweak the importance of the positional constraints.⁸ This leads to an over-determined system solved in the least-squares sense

$$(\tilde{L}^T \tilde{L})x = \tilde{L}^T \delta^{(x)} \quad (4)$$

Note that the coefficient matrix $A = (\tilde{L}^T \tilde{L})$ is now symmetric and positive definite, and totally determined once the set of indices of those constraint vertices is known, without their actual positions. In other words, the well known Cholesky factorization can be pre-computed just one time $(\tilde{L}^T \tilde{L}) = R^T R$. Then the system can be solved very efficiently by back substitution $R^T \xi = \tilde{L}^T \delta^{(x)}, Rx = \xi$, when the positions of the handle vertices are changed, which implies a change of the right-hand side vector.

Another advantage of using soft constraints is that we can use constraints on arbitrary points on the mesh. Note that each point on the mesh boundary surface is a linear combination of two or three vertices. For example, a point on an edge between vertices i and j is defined by $\hat{p}_{ij} = (1-\lambda)p_i + \lambda p_j, 0 \leq \lambda \leq 1$, thus can be employed as constraint by adding row of the form $(1-\lambda)x_i + \lambda x_j = \hat{p}_{ij}^{(x)}$ to the system. In other words, we can use some plane to cut the mesh surface to get some cutting points lie on some mesh edges, and generate a sketch contour curve to drive the deformation. In the following section, we will describe how to make use of the sketch contour driving deformation technique to do 3D rhinoplasty simulation, with operations as intuitive as those 2D image based simulation tools.

Surgery Planning and Simulation

The main workflow of the 3D rhinoplasty planning and simulation system is as following:

- (1) Reconstruct 3D models and generate the tetrahedral mesh of the facial soft tissue with inhomogeneous material.
- (2) Build an anatomical landmark system and do quantitative measurement of the nose.
- (3) Interactively plan and simulate the postoperative appearance of rhinoplasty using the specially designed deformation interface.
- (4) Automatically generate the patient specific prosthesis model if planning an augmentation rhinoplasty.

To aid in the exposition, we consider the first two steps as simulation preparing phase, and following two steps as surgical simulation phase. Then, we report some experiments and clinical validation results.

Prepare Simulation

When a patient needs to undergo a rhinoplasty surgery, a pre-operative CT scan is acquired and imported to the image processing and 3D reconstruction module of the system. First, highly detailed skin and bone surfaces are reconstructed, as shown in Figure 2(a,b). Then, a volumetric tetrahedral mesh is generated for the soft tissue region (including skin, muscle, fat tissue, and so on). Note that we restrict the tetrahedral mesh to the zone of the human face that may be influenced during rhinoplasty surgery to reduce processing time and memory usage, as illustrated in Figure 2(c).

The inhomogeneous material property assignment, e.g., the value of mesh element stiffness parameter m_k in Equation (3), is accomplished element-by-element by

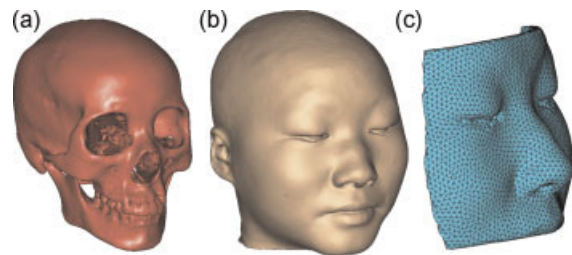


Figure 2. (a) Bone surface, (b) Skin surface, and (c) Volumetric mesh of soft tissue.

Soft tissue type	Range of CT HU value	Material stiffness (MPa)
Skin issue	-700 ~ -200	0.09 ~ 0.6
Muscle tissue	-50 ~ 250	0.5 ~ 0.8
Fat tissue	-200 ~ -50	0.001 ~ 0.01

Table 1. Range of CT HU value and material stiffness of different soft tissue type.

mapping CT scan values, just like the finite element modeling field. In more detail, the average grey scale value (HU: Hounsfield unit) of each mesh element is calculated and classified to different soft tissue types, as shown in Table 1, then mapped by linear interpolation to corresponding material stiffness.¹²

Subsequently, the anatomical landmark system is generated to quantitatively characterize the nose structure. First, the mid-sagittal plane of the head is determined semi-automatically, and used to generate a 2D section view of the head, such as demonstrated in Figure 3(a). Then, a group of landmarks are selected on the 3D skin and bone surfaces as well as on the 2D contours, such as the glabella, nasion, keystone and subnasal, based on which predefined anatomical measurements are automatically generated, including the nose height, nasofacial angle, nasomental angle, and so on, as in Figure 3(b). All these measurements are obtained in 3D and potentially provide more useful information to surgeons. In addition, some of the anatomical landmarks will be used to guide incoming simulation operations.

Surgical Simulation

The system provides several deformation tools to plan and simulate the postoperative appearance of rhinoplasty. The most interesting and intuitive tool is the

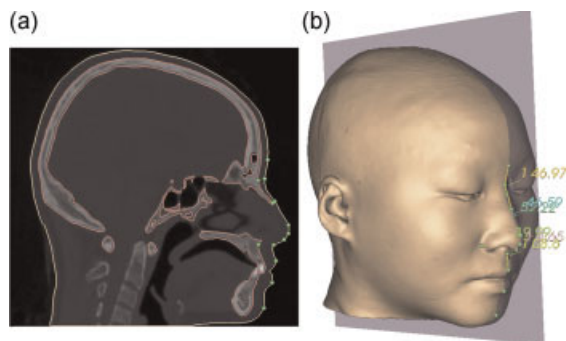


Figure 3. Anatomical landmark measurement system: (a) 2D section view by the mid-sagittal plane and (b) 3D view of anatomical measurements.

constraint sketch contour driving volumetric Laplacian deformation. Note that we do not simulate soft tissue deformation caused by bone osteotomy and/or prosthesis. Instead, the system employs a reverse simulation configuration to provide some kind of “what you see is what you get” effect, which is basically achieved by setting boundary conditions in a different way.

First, in the 2D view of mid-sagittal plane, the local section contour of the skin surface in-between the glabella and the subnasal point, called as *sketch contour*, is employed as the deformation handle of the soft tissue volumetric mesh. More precisely, the intersection points of the sketch contour with the outer surface of the volumetric mesh are used as handle points. Each point is the linear combination of two vertices of mesh edges, and processed as described in Section 3. To provide more convenient deformation control, the sketch contour is further approximated by a Spline control curve automatically, such as the blue curve shown in Figure 4(a), including all these in-between anatomical landmarks and some augmented points as control points (orange control balls). Then fixed conditions are defined by setting the stationary anchor vertices on the internal surface of volumetric mesh contacting the bone surface, except the local region of nose structure, such as illustrated in Figure 4(b). The local region of nose

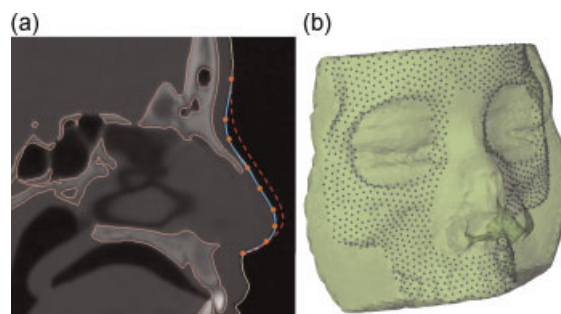


Figure 4. (a) Sketch contour in 2D view. The blue curve is the initial contour, which can be modified by the orange control points to new position, such as the red dotted curve. (b) Stationary anchor vertices on the internal surface of volumetric mesh.

structure is defined automatically by connecting several predefined landmarks on the bone surface.

On the algorithmic side, once the handle vertices and the stationary vertices are defined, the coefficient matrix $\tilde{L}^T \tilde{L}$ in (4) is totally determined and applied with Cholesky pre-factorization. Then, the control points of the sketch contour can be adjusted automatically according to some aesthetic statistical data, e.g., the ideal angles and proportions, or moved manually by the user, to modify the shape of the sketch contour and thereby to drive the deformation of the soft tissue mesh, such as illustrated in Figure 5(c). Each time the sketch contour is changed, the system is solved very efficiently by three back substitutions (for x, y and z separately) to reconstruct the deformation mesh almost in real-time, as shown in Table 2.

As mentioned in previous sub-section, for reasons of computational efficiency the volumetric mesh used for simulation is restricted to only the influenced zone of face, and is coarse due to the limited number of tetrahedrons. Moreover, since the perception of the human face is mainly determined by the relationship between different parts of the face, it is important for the surgeon to see the whole face and not just a part of it when inspecting the simulation result. Thus, it needs to map the deformation field of the sparse tetrahedral mesh to the detailed whole skin surface for a good

recognition, such as illustrated in Figure 5(e). We interpolate the deformation field by linear triangular shape functions. That is, during initialization each point of the skin surface (also restricted to only the influenced zone) is projected onto the outer triangular surface of volumetric mesh, and the corresponding triangle index and the barycentric coordinates (interpolation weights) are recorded. In the deformation stage, the displacement of every skin surface point is updated very efficiently by multiplying the interpolation weights to corresponding displacements of triangular surface vertices. The interpolation is also in real-time, as shown in Table 2, since only the outer surface of mesh is used.

The system also provides more free deformation tool, e.g., the user can select arbitrarily one or a group of handle vertices on the outer surface to drive the deformation, to reshape some asymmetric nose, or improve the result of sketch contour driving deformation. While, in practice the users rarely use it, as the constraint sketch contour driving deformation is so intuitive and straightforward to use.

Follow these scenarios, surgeons can simulate rhinoplasty surgery efficiently, and simultaneously patients feed back their suggestions to identify the desired outcome.

For simulation of augmentation rhinoplasty, when satisfied with the postoperative appearance, the change of soft tissue before and after simulation can be utilized

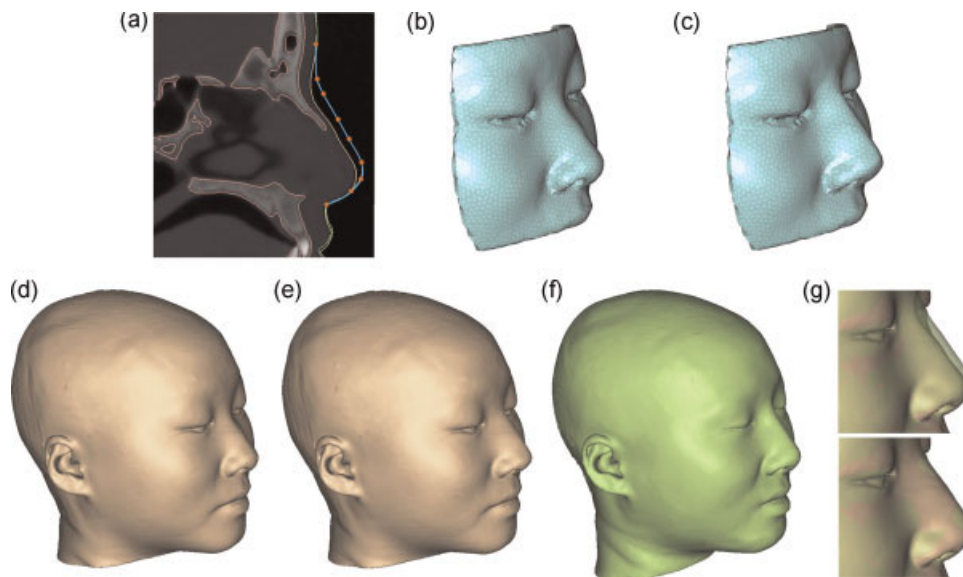


Figure 5. (a) Reshape the sketch contour according to the green section contour of post-operative skin surface, (b) Soft tissue volumetric mesh before deformation, (c) Soft tissue volumetric mesh after deformation, (d) Pre-operative skin surface, (e) Skin surface after deformation, (f) Real postoperative skin surface, and (g) Transparent post-operative surface is laid over the surface before and after deformation.

Data	Soft volumetric mesh			Skin surface		
	N_{tetra}	$T_{precompute}$	T_{update}	$N_{triangle}$	$T_{initialize}$	T_{update}
P1	19774	1781	78	90616	33	3
P2	18497	1697	77	99933	33	3
P3	21457	1811	88	110844	35	3
P4	28358	2454	109	130615	48	5
P5	33445	2759	162	153204	55	7
P6	22851	2064	92	125433	46	4
P7	19334	1698	76	101122	39	3
P8	35002	2963	171	206564	121	11
P9	20332	1810	85	128523	34	3
P10	29322	2662	125	143939	54	6

Table 2. Computation performance of the deformation method¹.

¹For soft volumetric mesh, N_{tetra} is the number of tetrahedra, $T_{precompute}$ is the Cholesky factorization time pre-computed once, and T_{update} is the interactive deformation time including three back substitutions. For skin surface, $N_{triangle}$ is the number of triangles, $T_{initialize}$ is the time for mapping initialization computed once, and T_{update} is the interactive interpolation time. All times are measured in milliseconds.

to design the patient specific prosthesis model. The basic idea is to deform the placement surface on which the prosthesis is put, by interpolating the deformation field of the soft tissue mesh, to generate a cave that needs to be filled with the prosthesis. However, this is not a trivial

task since the nasal cartilage is not distinguishable from the soft tissue in common CT scan. To address this problem, the system first generates the placement surface from local region of the pre-operative skin surface, such as illustrated in Figure 6(a). The offset

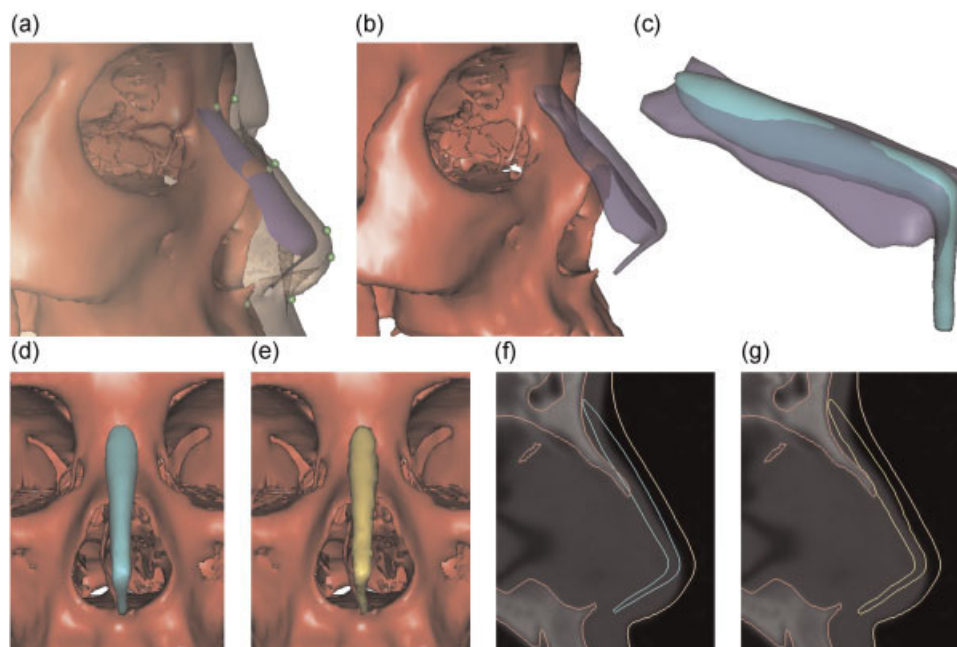


Figure 6. (a) Generate the placement surface on which the prosthesis is put, (b) Create the cave model by deforming a copy of the placement surface, (c) Design the patient specific prosthesis model by Boolean operation, (d, f) The final designed patient specific prosthesis model, and (e, g) The real prosthesis model reconstructed from the post-operative CT data.

distance at each vertex is interpolated from the distances between predefined landmarks, such as the keystone points on skin and bone, as well as some statistical data about the thickness of nasal soft tissue. Following, a copy of the placement surface is deformed by interpolating the soft tissue deformation field, using tetrahedral shape functions, forming a cave model, as in Figure 6(b). Then, a standard nose prosthesis model is chosen and overlaid on the cave model, as in Figure 6(c), to generate the patient specific prosthesis model, as shown in Figure 6(d) and (f), by a Boolean operation and some smooth operations at the cut edges and two sides on the width direction.

Finally, some post-operative measurements can be done, compared with the pre-configurations, and the surgical plan can be made according to the simulation results. In addition, the designed prosthesis model can be exported to some rapid prototyping equipment to generate the physical patient specific prosthesis if planning an augmentation rhinoplasty.

Experiment and Clinical Validation

Before a plastic simulator can be used in routine clinical practice, it has to be shown that this simulator is able to give an accurate prediction of the new facial outlook after surgery. The only way to truly measure this accuracy is by comparing the post-operative data with the predicted data. We have collected a database of 10 patients who underwent an augmentation rhinoplasty procedure, with pre-operative as well as post-operative CT data.

For each patient data, the detailed skin and bone surfaces, and the soft tissue mesh from the pre-operative CT were generated as before. Following, the skin and bone surfaces from the post-operative CT were also

reconstructed, and transformed to the coordinate system of the pre-operative CT data, by registration of the bone surfaces using ICP algorithm. Then, the surgical simulation was done on pre-operative data as previous section. Specifically, the sketch contour to drive deformation was reshaped according to the section contour of the registered post-operative skin surface, such as demonstrated in Figure 5(a). Then, the predicted skin surface after deformation, shown in Figure 5(e), could be compared with the real post-operative skin surface, shown in Figure 5(f) and (g). If planning an augmentation rhinoplasty, the designed individual prosthesis model could also be compared with the real one from post-operative CT, as in Figure 6(e) and (g). Note that for quantitative measurement of distances between the predicted and post-operative skin surfaces, only the deformed part of the surface, except the eye region, were included for statistics. The statistical results for the differences of skin surfaces demonstrated that the mean vertex difference was below 0.1 mm, the average 90% percentile was below 1 mm, and the average peak difference was about 1.8 mm, which usually located near the nasal orifices. For the patient specific prosthesis models, the statistical results demonstrated that the system designed models have a good fit for the thickness of prosthesis, as shown in Figure 6(f) and (g), with the mean difference about 0.1 mm, and the average peak difference about 1.5 mm. For the widths of prosthesis, the system designed models were usually larger than real models, with the mean difference about 0.2 mm and the average peak difference about 2 mm. While, according to clinical surgeons, the thickness is much more relevant than the width of prosthesis for nose surgery. Figure 7 illustrates simulation results of another patient data.

Table 2 reported the computation performance of our deformation method. All calculations were performed

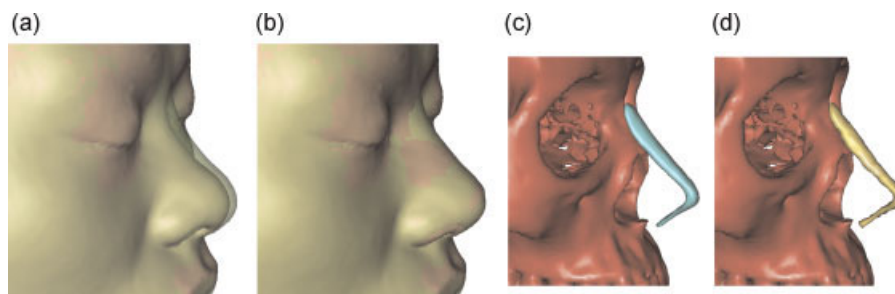


Figure 7. (a) Pre-operative skin surface with transparent real post-operative surface, (b) Skin surface after deformation with transparent post-operative surface, (c) The final designed patient specific prosthesis model, and (d) The real prosthesis model reconstructed from the post-operative CT data.

on a standard desktop computer with Intel Pentium Core 2 Duo processor running at 2×2.83 GHz and 4 Gbyte RAM. We can see that the most time consuming procedure is the Cholesky factorization for the soft tissue volumetric mesh deformation, while, this is done only once when the sketch contour and the stationary vertices are defined, and yet usually only costs less than 3 seconds. During interactive simulation, each time the sketch contour is changed, the system only costs less than 0.2 second to reconstruct the deformation mesh, and the time for mapping the deformation to the skin surface can be almost ignored. Thus the surgery simulation can be performed at a high interactive frame rates.

Finally, as the use of finite element method (FEM) has been regarded as the benchmarking method for biomechanical simulation, we did some comparing experiments. In more detail, once the surgical simulation using our system was done, the same soft tissue volumetric mesh model, inhomogeneous material property, and boundary conditions (fixed and moved handle vertices) were exported to FEM system ANSYS 10 (ANSYS Inc.) for simulations. Figure 8(a) illustrates a FEM simulation result. Note that in the region surrounding the ridge of nose (with blue arrows), the

deformation is unnatural and non-smooth. In contrast, the simulation produced by our volumetric Laplacian method has much better match to the real post-operative surface as shown in Figure 8(b). The reason is that in this paper the sketch contour is used to drive deformation, e.g., with a small number of handle vertices along the ridge of the nose, which is not the real physical boundary condition caused by bone osteotomy and/or prosthesis. In addition, it took more than 4 minutes for FEM to finish deformation.

We also implemented the gradient-based volumetric deformation approach,¹¹ as expected, resulting similar non-smooth deformation result in the ridge of the nose as FEM. In fact, the Laplacian based method actually solves a normal system of order 2 instead of order 1 as the gradient-based method as well as FEM, leading to smoother deformation between the handle and fixed constraint region, which is important for the use of sketch contour with very sparse handle vertices to drive deformation, thus more suitable for the reverse simulation configuration in this paper.

Conclusion

This paper presents an intuitive computer assisted nose surgery planning and simulation system, which is designed with practical motivation to achieve some kind of “what you see is what you get” function. Based on the symmetric characteristic of the nose structure, the system exploits a special sketch contour driving deformation interface, which can provide realistic 3D rhinoplasty simulation with straightforward 2D manipulation. The key component underlying the system is a novel volumetric Laplacian deformation method inspired by the state-of-the-art differential surface deformation techniques. Working on the volumetric domain and incorporating inhomogeneous material make the new deformation approach suitable for soft tissue simulation. The system also provides function to design the patient specific prosthesis model, which can further be exported to some rapid prototyping equipment to create the real physical individual prosthesis. Compared to existing rhinoplasty simulation systems, these tools are more convenient for the communication between surgeons and patients to identify the desired outcome of surgery, and more useful to put the simulation result into actual use.

We also acknowledge the limitations of our study. First, the deformation method does not directly support tissue cutting and suturing,¹³ although not required in

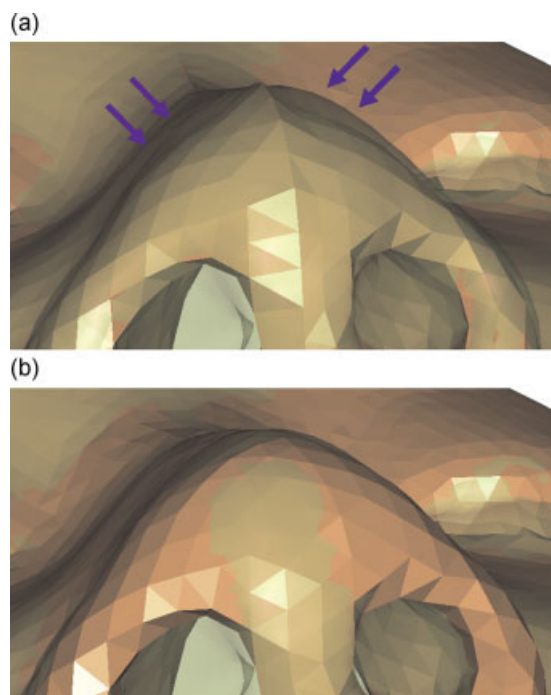


Figure 8. (a) Deformation using finite element method, with transparent real post-operative surface and (b) Volumetric Laplacian method.

current simulation system. Second, it is essentially a geometric method, although taking physical material into consideration; and we intend to consider more physical based way in the near future.¹⁴

Anyway, clinical quantitative validation using post-operative CT data demonstrated that the system can provide prediction results of high quality. In addition, the soft tissue simulation can be interactively performed almost in real-time, which is also a major concern to develop practical simulation systems from the point of clinical view. We also had a group of qualitative validations, the surgeons who used the system confirmed that this planning and simulation system is very attractive and has potential for daily clinical practice. We intend to have more clinical validation to improve the simulation system in the near future, and incorporate tightly some hardware equipment to form a complete nose surgery planning and simulation system for clinical application.

ACKNOWLEDGEMENTS

The research was supported by the National Natural Science Foundations (No. 60903136, No. 60873126), the Doctorial subject special scientific research fund of Education Ministry (20070335074), and the Postdoctoral Science Foundation (20080441236) of China.

References

1. Nealen A, Müller M, Keiser R, *et al.* Physically based deformable models in computer graphics. *Computer Graphics Forum* 2006; **25**(4): 809–836.
2. Irving G, Teran J, Fedkiw R. Invertible finite elements for robust simulation of large deformation. In *Eurographics Symposium on Computer Animation*, 2004; 131–140.
3. Ozkul T, Ozkul MH. Computer simulation tool for rhinoplasty planning. *Computers in Biology and Medicine* 2004; **34**: 697–718.
4. Kavagiou Z, Bello F, Scott G, *et al.* Facial plastic surgery planning using a 3D surface deformation tool. *Studies in Health Technology and Informatics* 2005; **111**: 247–250.
5. Lee T-Y, Lin C-H, Lin H-Y. Computer-aided prototype system for nose surgery (Rhinoplasty). *IEEE Transactions on Information Technology in Biomedicine* 2001; **5**(4): 271–278.
6. Botsch M, Sorkine O. On linear variational surface deformation methods. *IEEE Transactions on Visualization and Computer Graphics* 2008; **14**(1): 213–230.
7. Yu Y, Zhou K, Xu D, *et al.* Mesh editing with poisson-based gradient field manipulation. *ACM Transactions on Graphics* 2004; **23**(3): 644–651.

8. Sorkine O, Cohen-Or D, Lipman Y, *et al.* Laplacian surface editing. In *Eurographics Symposium on Geometry Processing*, 2004; 175–184.
9. Meyer M, Desbrun M, Schroder P, *et al.* Discrete differential-geometry operators for triangulated 2-manifolds. In *Visualization and Mathematics III*, Hege H-C, Polthier K, (eds). Springer: Heidelberg, 2003; 35–57.
10. Wang Y, Gu X, Yau S-T. Volumetric harmonic map. *Communications in Information and Systems* 2004; **3**(3): 191–202.
11. Liao S-H, Tong R-F, Dong J-X. Gradient, Field based inhomogeneous volumetric mesh deformation for maxillo-facial surgery simulation. *Computers and Graphics* 2009; **33**: 424–432.
12. Schnabel JA, Tanner C, Smith AD, *et al.* Validation of non-rigid registration using finite element methods. *Lecture Notes in Computer Science* 2001; **2082**: 344–357.
13. Sifakis E, Der K, Fedkiw R. Arbitrary cutting of deformable tetrahedralized objects. In *Eurographics Symposium on Computer Animation*, 2007; 73–80.
14. Yan H-B, Hu S-M, Martin RR. 3D morphing using strain field interpolation. *Journal of Computer Science and Technology* 2007; **22**(1): 147–155.

Authors' biographies:



Sheng-hui Liao received the B.S. degree in 2003 and Ph.D. degree in 2008 at Department of Computer Science and Engineering from Zhejiang University, China. From 2008, he continued his research as a postdoctoral researcher at Zhejiang University and currently he is an assistant research fellow. His research interests include medical image analysis, computer-aided surgery, biomechanical modeling and analysis, and machine learning.



Ruo-feng Tong received the B.S. degree in Mathematics from Department of Mathematics, Fudan University in 1991 and Ph.D. degree in Mathematics in 1996 from

Department of Mathematics, Zhejiang University, China. He continued his research as a postdoctoral researcher at Intelligent Systems and Modeling Laboratory, Hiroshima University, Japan. Currently, he is a Professor at Department of Computer Science and Engineering, Zhejiang University, China. His research interests include CAD/CG, and computer animation.

Jian-Ping Geng received his first postdoctoral training in Dentistry at National University of Singapore and second postdoctoral training in Clinical Surgery at Zhejiang University. Currently, he is a professor at Institute for Biomedical Engineering, Nanjing University of Tech-

nology. His research interests include computer-aided surgery, biomechanical modeling and analysis, and medical image analysis.

Min Tang received the B.S. degree in 1994 and Ph.D degree in 1999 at Department of Computer Science and Engineering from Zhejiang University, China. Currently, he is an associate professor at Zhejiang University. He is a visiting scholar at the Department of Computer Science, Wichita State University in 2006, and at the Department of Computer Science, UNC-Chapel Hill in 2008. His research interests include CAD/CG, system integration, and physical modeling.